ARTICLE   OPEN

Bringing sensation to prosthetic hands—chronic assessment of implanted thin-film electrodes in humans

Paul Čvančara [1✉], Giacomo Valle [2,3], Matthias Müller[1], Inga Bartels[1], Thomas Guiho [4], Arthur Hiairrassary[4], Francesco Petrini[2], Stanisa Raspopovic[2,14], Ivo Strauss [2,3], Giuseppe Granata[5], Eduardo Fernandez[6], Paolo M. Rossini[5,7], Massimo Barbaro[8], Ken Yoshida[9], Winnie Jensen[10], Jean-Louis Divoux[11,15], David Guiraud [4], Silvestro Micera [2,3] and Thomas Stieglitz [1,12,13]

Direct stimulation of peripheral nerves with implantable electrodes successfully provided sensory feedback to amputees while using hand prostheses. Longevity of the electrodes is key to success, which we have improved for the polyimide-based transverse intrafascicular multichannel electrode (TIME). The TIMEs were implanted in the median and ulnar nerves of three trans-radial amputees for up to six months. We present a comprehensive assessment of the electrical properties of the thin-film metallization as well as material status *post explantationem*. The TIMEs stayed within the electrochemical safe limits while enabling consistent and precise amplitude modulation. This lead to a reliable performance in terms of eliciting sensation. No signs of corrosion or morphological change to the thin-film metallization of the probes was observed by means of electrochemical and optical analysis. The presented longevity demonstrates that thin-film electrodes are applicable in permanent implant systems.

INTRODUCTION

Several research groups developed technological solutions to provide sensory feedback for bidirectional prosthetic limb control[1–4] to reduce rejection of prosthesis use[5,6], improve user's quality of life and increase dexterity[1,2,7–11] as well as embodiment with a positive impact on that distressing condition named phantom limb pain (PLP)[8,12,13]. In order to achieve optimal performance, peripheral nerve interfaces (PNIs) need to exhibit high spatial resolution, must show a limited foreign body reaction and must not exceed the electrochemical safe limits of stimulation[14]. Needless to say, that longevity and technical stability of the implanted devices are key to success in all studies, no matter which PNI design has been chosen. The ideal vision for the amputee would be a replacement of the missing limb with a sensorized prosthesis, which is connected to such an interface and gives the patient sensory feedback[6]. Therefore, chronic stability of implanted PNIs is the ultimate prerequisite. By now, a limited amount of PNIs proved stability over long implantation periods[15,16] in the range of years.

The first successful approach was introduced by Dhillon and co-workers[17] with longitudinal intrafascicular electrodes (LIFE) implanted in human subjects subchronically. The drawback of the original LIFE concept is the low spatial stimulation selectivity with only one contact per wire. To overcome this drawback, polyimide (PI) based thin-film longitudinal intrafascicular flexible electrodes (tf-LIFE) with a higher number of stimulation sites were developed and implanted subchronically into a human upper limb amputee[18]. Unfortunately, the foreign body reactions around the implant drove stimulation thresholds into the maximum safe

charge injection limit after two weeks and the stimulation had to be stopped.

One of the simplest, very stable, common PNIs is the cuff electrode, which is implanted circumferentially around the targeted nerve. Cuffs are very robust, but with limited excitation capabilities of the inner fascicles of a nerve and therefore limited in spatial selectivity[19]. To overcome this drawback Tyler & Durand developed the flat interface nerve electrode (FINE, manufactured with silicone rubber molding and spot welding)[20], which flattens and re-arranges the nerve for higher selectivity. Attention has to be payed to the force applied[21]. The FINE was successfully implanted chronically up to 3.3 years in the median and ulnar nerves of upper limb amputees[2,22].

Multi-channel microelectrode arrays (MEAs) based on silicon needles[23] and shanks[24] were initially developed for intracortical application. Modified MEAs were subchronically tested in human median and ulnar nerve of upper limb amputees for four weeks[25]. Barrese et al. showed, that not only biological reasons like gliosis lead to failure of intracortical MEAs, but also material and mechanical causes[26]. They investigated the device stability on 78 chronically implanted devices in non-human primates via analysis of the signal recordings. 62 devices (i.e. 79%) failed entirely and most of the failures occurred within the first year of implantation due to mechanical issues, particularly due to failures within the connector. A complete signal loss for all implants was predicted by about 8 years. Within a further study, Barrese et al. investigated eight MEAs implanted chronically in eight non-human primates using scanning electron microscopy (SEM)[27]. They observed several technical failure modes: corrosion of the

[1]Laboratory for Biomedical Microtechnology, Department of Microsystems Engineering – IMTEK, Albert-Ludwig-University Freiburg, Freiburg, Germany. [2]Center for Neuroprosthetics and Institute of Bioengineering, School of Engineering, École Polytechnique Fédérale de Lausanne (EPFL), Lausanne, Switzerland. [3]The Biorobotics Institute, Scuola Superiore Sant'Anna, Pisa, Italy. [4]Camin Team, INRIA, University of Montpellier, Montpellier, France. [5]Institute of Neurology, Catholic University of the Sacred Heart, Roma, Italy. [6]Institute of Neurosurgery, Catholic University of the Sacred Heart, Roma, Italy. [7]Polyclinic A. Gemelli Foundation-IRCCS, Roma, Italy. [8]Department of Electrical and Electronic Engineering, University of Cagliari, Cagliari, Italy. [9]Biomedical Engineering Department, Indiana University-Purdue University, Indianapolis, IN, USA. [10]SMI, Dept. Health Science and Technology, Aalborg University, Aalborg, Denmark. [11]AXONIC / Groupe MXM, Vallauris, France. [12]BrainLinks-BrainTools, Albert-Ludwig-University Freiburg, Freiburg, Germany. [13]Bernstein Center Freiburg, Albert-Ludwig-University Freiburg, Freiburg, Germany. [14]Present address: Laboratory for Neuroengineering, Department of Health Sciences and Technology, Institute for Robotics and Intelligent Systems, ETH Zürich, Zürich, Switzerland. [15]Present address: A!MD: Advice In Medical Devices, Paris, France. ✉email: paul.cvancara@imtek.uni-freiburg.de
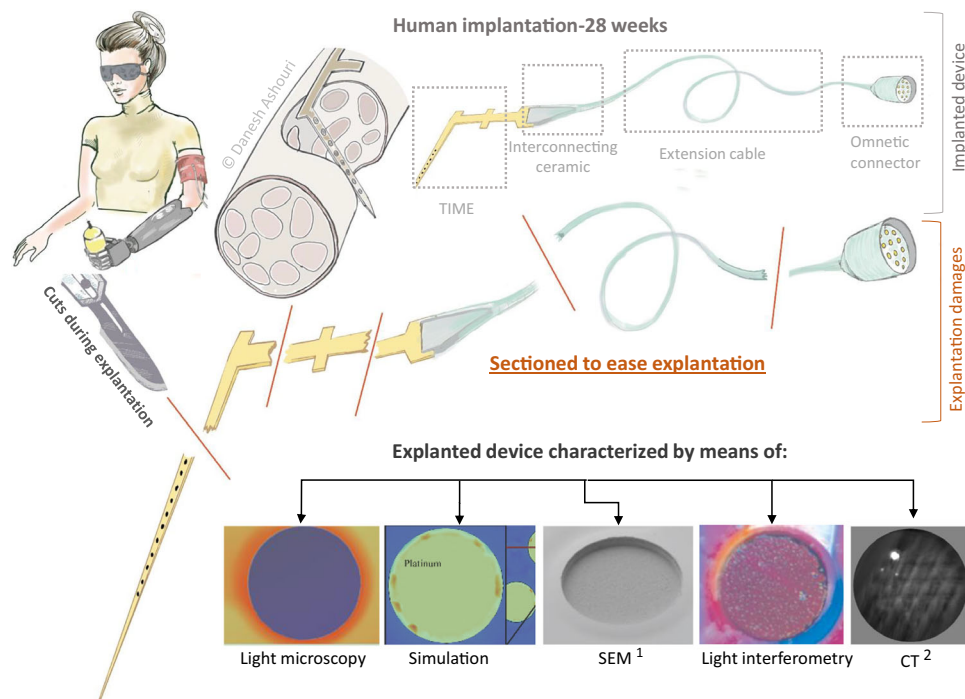
Fig. 1 Analysis methods of TIME. Functional performance was evaluated in vivo by questionnaires and impedance measurements. After termination of the clinical study, TIMEs got explanted and percutaneous cables and parts and pieces of the micromachined foils with embedded electrodes were analyzed by light microscopy, [1]scanning electron microscopy (SEM), white light interferometry and micro [2]computing tomography (CT).

platinum electrode tips occurred, as well as changes to the underlying silicon bulk material. Moreover, the protective insulation materials like parylene-c and silicone elastomer exhibited defects. The parylene-c was susceptible to crack formation and therewith delamination. Silicone elastomer used for device insulation delaminated at edges. The materials defects accumulated with time in vivo. These results showed that long-term stability of devices is an absolutely mandatory requirement for chronic usage and patient safety of (active) implants.

In terms of spatial selectivity polyimide (PI) based transverse intrafascicular multichannel electrodes (TIME)[28] have shown very promising results[19], as they are pulled through the nerve and can address as well the inner fascicles maintaining a steady contact-to-fascicle relationship in time. After verification in vitro and in vivo within small and large animal models[19,29–31], PI-based thin-film implants[18] and TIMEs showed good subchronic clinical performance[1,32]. Use of iridium oxide as stimulation contact material with its high charge injection capacities kept the stimulation sites well in the chemically safe regime over increasing thresholds caused by the foreign body reaction period. TIME assessment after the first-in-human study[33] which covered a time period of 30 days and showed signs of severe adhesion loss led to inclusion of a silicon carbide adhesion layer. Stability was verified in a rodent study for one month as prerequisite to enter further clinical studies on humans[7–9,13,34–36]. Within this study, we present the analysis of implants used in the mentioned clinical studies implanted for up to six months.

RESULTS

Design changes, incorporation of adhesion layers and improvements of packaging and assembly increased stability and longevity, which is mandatory to head towards a fully implantable system for long-term use of years. Assessment of electrical performance in vivo was associated to in depth analysis of explanted TIMEs (Fig. 1) by microscopic analyses methods. In this

study we showed the feasibility of implanting thin-film electrodes for long-term applications in human. We are confident in longevity of thin-film electrodes and in the feasibility of polyimide-based permanent implants if the whole system design is long-term stable as such.

Simulation of intrinsic mechanical stress in different ground contact designs

Ground contact sites are of fundamental importance in stimulation devices, as a failure would lead to a total malfunction of the implant. Current is injected over an active site (source) while the ground electrode closes the electrical circuit (sink). Observations in previous studies indicated the need of a redesign of the previously used rectangular large area ground (GND) contact sites due to adhesion failure and integrity loss[14,33]. The aim of the redesign was to prevent stress due to the large continuous area and rectangular edges (1 mm × 0.25 mm; $A = 0.25$ mm^2), but to keep an area as large as possible to ensure an electrical feedback-loop with low current density for stimulation. To preserve these boundary conditions, the rectangular ground site was split to 109 interconnected circular contacts with an exposed diameter of $d = 80$ μm (Fig. 2) (diameter under polyimide $d = 100$ μm) of a single site. The contacts were arranged in a hexagonal assembly with a pitch of 125 μm in three rows.

The simulation of thermally induced stress due to the steam sterilization process (121℃, 2 bar) using COMSOL Multiphysics® (version 5.3, COMSOL Inc., Burlington, MA, USA) was run with both design approaches, a rectangular large area ground contact and a split ground with 109 circular interconnected contact sites (Fig. 2).

The van Mises stress level was indicated with a color range from low stress in blue to high stress in red. Generic, the stress was calculated in the middle of the rectangular ground contact superficial of the thin-film metallization within a low-stress area (indicated by the dashed black line, Fig. 2a) with a length of 1 mm and with a distance of 8 μm from the edge of the polyimide in a
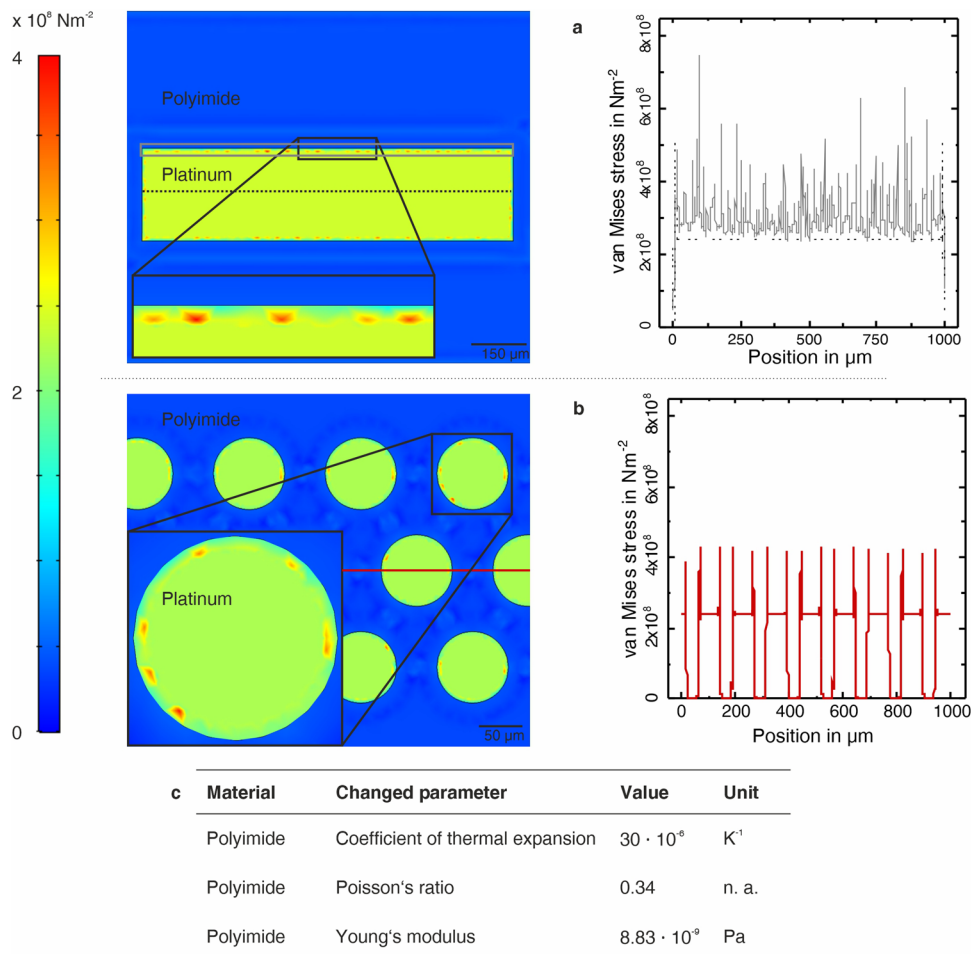
Fig. 2 Simulation of thermal induced stress of different ground contact approaches. a The rectangular ground contact site (1 mm × 0.25 mm) was used on the TIME-3H within a subchronical trial[33]. Simulated stress values were acquired close to the edge of the PI (grey line) and in the middle of the contact (dashed line). **b** The split ground with 109 single redundant connected contact sites (diameter of single contact 80 μm) was designed for chronic application. **c** Simulated stress values were acquired in the middle of the device on a length of 1 mm. Several standard parameters of the simulation software for the thermo-mechanical stress simulation of various ground contact sites were changed.

high-stress area (indicated by the grey box, Fig. 2a). In the low-stress segment, the stress did not exceed $2.4 \cdot 10^8$ Nm^{-2}, except at the edges (Position 0 μm and 1000 μm). In the high stress segment, the simulated van Mises stress was constantly above $2.4 \cdot 10^8$ Nm^{-2}, with peaks up to $7.5 \cdot 10^8$ Nm^{-2}. The integrated van Mises stress over the length of 1000 μm resulted in $3.0 \cdot 10^{11}$ Nm^{-1} for the high stress segment, and $2.4 \cdot 10^{11}$ Nm^{-1} for the low stress segment.

For the split ground contact, the simulated van Mises stress was calculated along the indicated red line with a length of 1 mm (Fig. 2b). Peaks with a maximum stress of $4.3 \cdot 10^8$ Nm^{-2} occurred at the edges of the exposed single contacts. Between the exposed thin-film metallization thus where the metallization was sandwiched between two polyimide layers, the stress dropped entirely. At other exposed metallization surfaces the stress stayed constant like above at $2.4 \cdot 10^8$ Nm^{-2}. The integrated van Mises stress over the length of 1 mm resulted in $1.6 \cdot 10^{11}$ Nm^{-1}. Summing, while peak magnitudes stayed in similar ranges, the spatial extent of high-stress regions was much smaller.

Electrochemical characterization of thin-film electrodes in vivo (human arm nerves)

Twelve TIME implants of the latest generation were implanted in the median and ulnar nerves of three patients for up to six months

(details of implantation and can be found elsewhere[7]). The performance of the TIME implants was measured in terms of impedance (details can be found in the methods section) of each stimulation contact. The impedance was acquired weekly for every patient during the clinical trials (Fig. 3a). The impedances of the implants used for patient 1 were from the beginning close to 100 kΩ. With a moderate slope of 0.8 kΩ per week the impedances reached a plateau a little higher than 100 kΩ already in week 5. After week 22 a strong decrease in impedance occurred, reaching a mean impedance of 73 kΩ ± 18 kΩ close to termination of the clinical trial. The mean impedance of the devices of patient 2 was in the first week after implantation at a very low level of 21 kΩ ± 26 kΩ. From week 11 on, the impedances stabilized on a plateau of about 100 kΩ, resulting in a slope of 2.8 kΩ per week. The mean impedance of the implants of patient 3 increased from 60 kΩ ±36 kΩ in week 1 moderately to 67 kΩ ±36 kΩ, at the end of the trial resulting in a slope of 0.8 kΩ per week. In contrast to patient 1, there was no plateau in the middle of the clinical trial.

Prevention of nerve damage was of the highest priority during the explantation procedure. Therefore, all cables were cut and the connector was removed before the explantation of the intrafascicular device was accessed. Due to these circumstances we were not able to conduct sophisticated electrochemical analysis of the electrode contacts after explantation. The thin-film parts of the

a

b

c
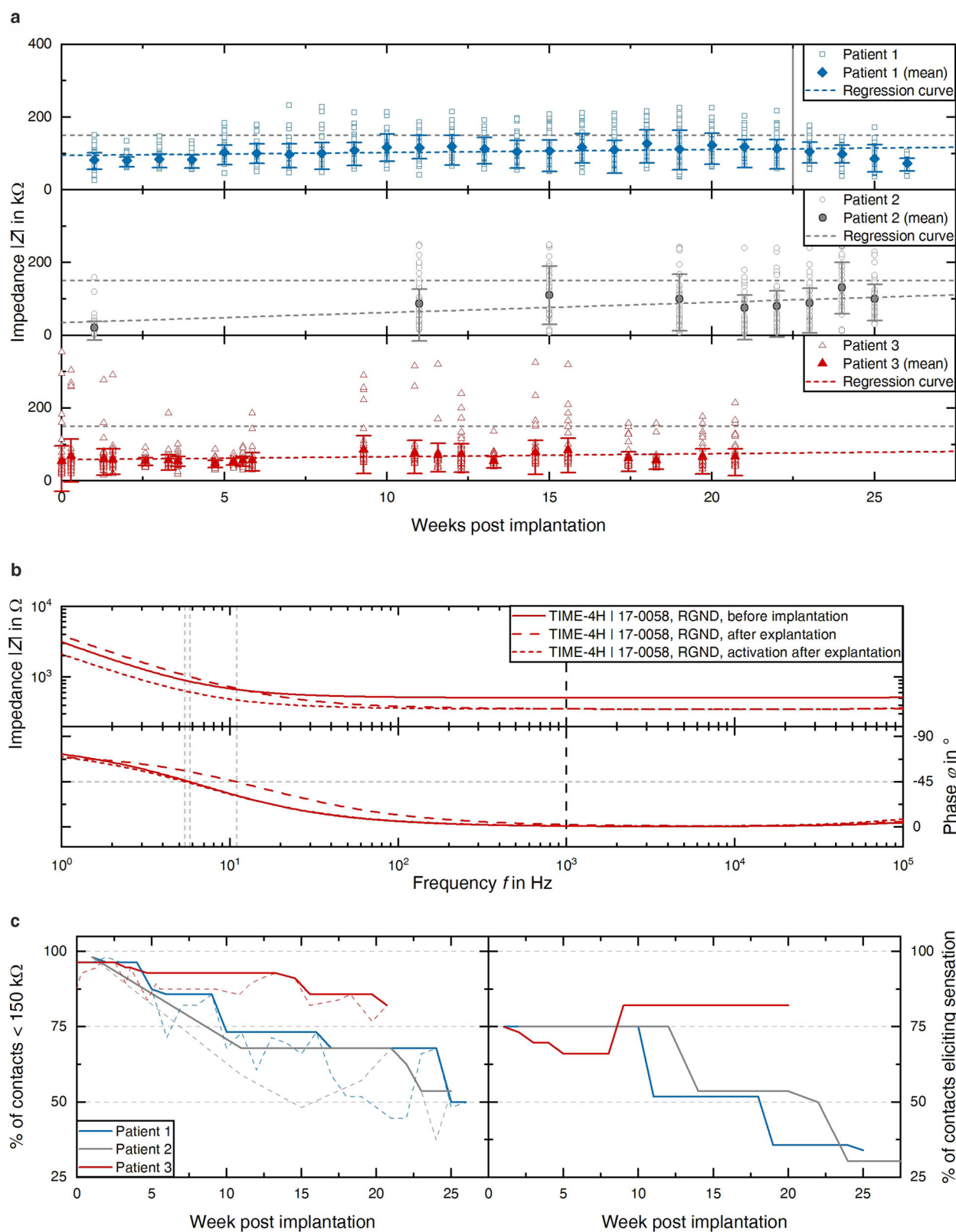
implants had to be removed from the nerve carefully not to harm the patient. During explantation and handling after explantation all contacts but one ground contact were electrically disconnected. This single right ground contact (serial number TIME-4H | 17-0058, patient 3, ulnar nerve, proximal position) was characterized after explantation via electrochemical impedance spectroscopy (EIS, Fig. 3b). The impedance at 1 kHz decreased from 508 Ω before implantation to 355 Ω after explantation. Subsequently, the implant was hydrated using cyclic voltammetry. Further EIS displayed an impedance of 354 Ω at 1 kHz. The cut-off

Data from electrochemical analysis in vivo and in vitro. a Evolution of impedance measured in vivo during the clinical trial of all patients. Transparent objects represent the single recorded values, filled objects represent the mean value of all contact on the day of measurement. The regression curve (linear mixed model estimate) was evaluated using a linear mixed effect model. For patient 1, the estimated intercept was 94.34 kΩ, slope 0.8 kΩ per week, F-value 43.1368 and p value < 0.0001. For patient 2, the estimated intercept was 34.77 kΩ, slope 2.8 kΩ per week, F-value 57.69014 and p value < 0.0001. For patient 3, the estimated intercept was 57.95 kΩ, slope 0.8 kΩ per week, F-value 39.95188 and p value < 0.0001. **b** Characterization of the right ground contact of the implant with the serial number TIME-4H│17-0058 before implantation and after explantation (number of contacts investigated: one). Following a first characterization after explantation, the implant was hydrated and again characterized. **c** Kaplan-Meier-Plot comparing the percentage of electrically functional stimulation contacts (impedance <150 kΩ) between the three chronic patients (left). Dashed lines display the real measured contact with fluctuation, within the continuous lines the fluctuation was filtered. Beyond, the percentage of contacts eliciting sensation reported by the patients was acquired over the time of implantation (right).

frequency increased from 5.8 Hz before implantation to 11 Hz afterwards. The hydration led to a decrease to 5.4 Hz.

An electrically well-functioning stimulation contact site was defined having an estimated in vivo impedance of <150 kΩ. With this definition, we analyzed the course of electrically functional contact sites in percentage over time in weeks postimplantation (Fig. 3c, left). The dashed lines represented the real measured percentage, including fluctuation. The continuous lines ignored the fluctuation and visualized the highest effective percentage. The TIMEs used for patient 1 and 2 had a loss of electrically functional contacts from initial 98.2% down to 73%, respectively 68% after 11 weeks. During the remaining course of the trial, a further decrease to a final 50%, respectively 54% could be observed. The percentage of electrically functional contacts of the devices implanted in patient 3 dropped from 96% after week 1 to 82% at the end of the clinical trial.

Next to the objective acquisition of electrically functional contacts, a subjective assessment of stimulation contact eliciting sensation was performed (Fig. 3c, right). Patient 1 felt until week 10 75% of the contacts eliciting sensation, patient 2 until week 12. For both in the course of the clinical trial the percentage dropped to 34% and 30%, respectively. Patient 3 communicated in the beginning (also starting at 75%) a drop, with a stabilization after week 9 at 82%, persistent until the end of the clinical trial.

Optical analysis of explanted thin-film electrodes

The impedances of the implanted TIMEs were recorded until the last day of the clinical trial, prior to explantation. Following explantation, the implants were optically analyzed in detail after thorough cleaning. The available data from the optical analysis (111 stimulation contact sites out of 168 implanted) were compared to the recorded impedance data close to explantation. The impedances (Fig. 4a) of the stimulation contact sites were linked with the optically analyzed status to five categories, from category 1 (like pristine) up to category 5 (heavy delamination of > 6 μm, disintegration of the metallization layers or compression or destruction of the PI substrate) (Fig. 4b). Details can be found in the Methods section.

Could a certain impedance range be assigned to a classification of mechanical damage? An optically and mechanically pristine contact site corresponding to category 1 should exhibit a low impedance (<150 kΩ), whereas an entirely destroyed contact site with for example missing metallization and corresponding to category 5 should either exhibit a very high impedance or even not be measurable.

The median impedances of all categories were between 46 kΩ and 79 kΩ (Fig. 4c), thus within the definition of an electrically functional stimulation contact site (<150 kΩ). The same applied for the median values, which were even in a narrower band of 50 kΩ to 67 kΩ. The majority of the impedance with 82% came under category 1 to 3. Only 7%, respectively 11% were related to category 4 and 5. In Fig. 4c the data was summarized.

A non-parametric Kruskal-Wallis method was applied to assess differences between the impedances of the categories (Fig. 4a).

The categorized impedances displayed no statistically significant difference at the α-level of 0.05.
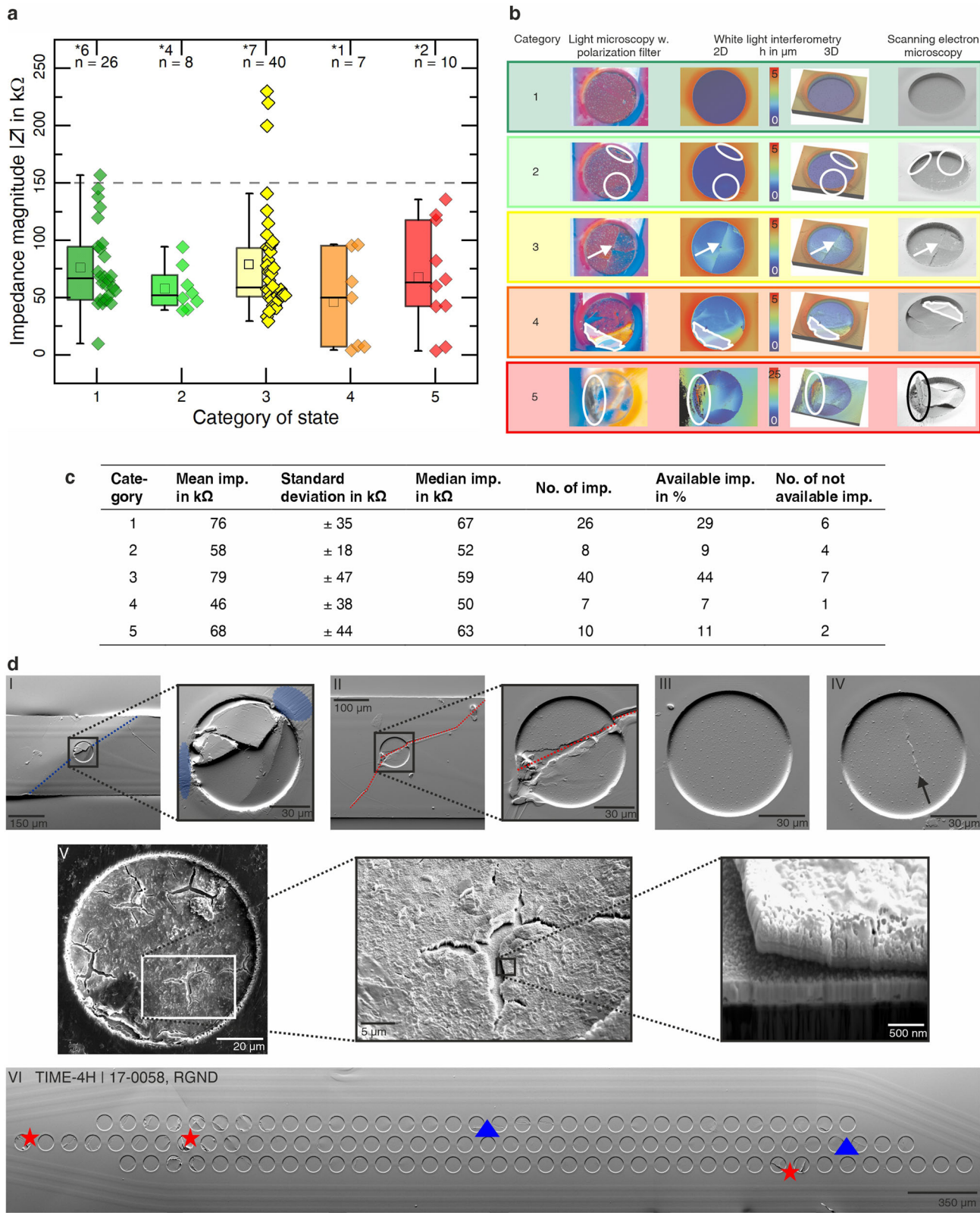
Detailed images of the stimulation contact sites (111 out 168 available) were acquired using SEM. Especially on contact sites classified in category 5, traces of external mechanical impacts could be detected (Fig. 4d). The failure causes were associated to mechanical interactions during handling. The PI thin-film in Fig. 4dI) was bended heavily alongside the dashed blue line, resulting in total destruction of the metallization within the contact site. Groove marks in the PI resulting from the bending were highlighted with blue elliptic markers. A further mechanical impact originated from an object, which scratched the surface of the PI substrate and the thin-film metallization (Fig. 4dII), dashed red line). The detailed image revealed heavy damage to the thin-film metallization. In total 10 out of 12 optically analyzed category 5 stimulation contact sites exhibited distinct signs of external mechanical impacts. Ten exhibited impedances <150 kΩ, while further two were not measurable. As already stated above, all implants were fully functional at the time point of delivery. A stimulation contact site from category 1 did not show any negative optical effect (Fig. 4dIII). It exhibited on the last day of the clinical trial an estimated impedance of |Z| = 138.3 kΩ. A stimulation contact from category 2 exhibited slight crack formation without any negative effect on the stimulation parameters as it exhibited an impedance of |Z| = 94.2 kΩ (Fig. 4dIV).

For comparison reasons, identical stimulation contact designs to the TIME devices were stimulated with up to 6.5 billion pulses in vitro which would correspond to more than 200 days of continuous stimulation at 50 Hz or years of intermittent stimulation depending on the protocol. After 4.5 billion pulses first morphological changes could be observed within one contact, which expressed as trident crack formation with a length of about 20 μm (Fig. 4dV).

Overview images of the ground contact sites were acquired after explantation, cleaning and when possible after electrochemical analysis. The implant with the serial number TIME-4H│17-0058 was implanted in the proximal position of the ulnar nerve of patient 3. After explantion, it was electrochemically characterized using EIS (Fig. 3b) and exhibited an impedance of 354 Ω at 1 kHz. Thereafter, SEM images were acquired (Fig. 4dVI). Approximately 50% of the single-ground contact sites displayed cracking or even partial delamination. Indicated by a red star, crack formation with partial delamination is shown. A slight crack formation is indicated by the blue triangles. More overview images of the ground contact sites can be found in the supplementary material. Predominantly, all via optical methods investigated ground contacts were mechanically intact, though they also displayed a certain amount of mechanical damage within the thin-film.
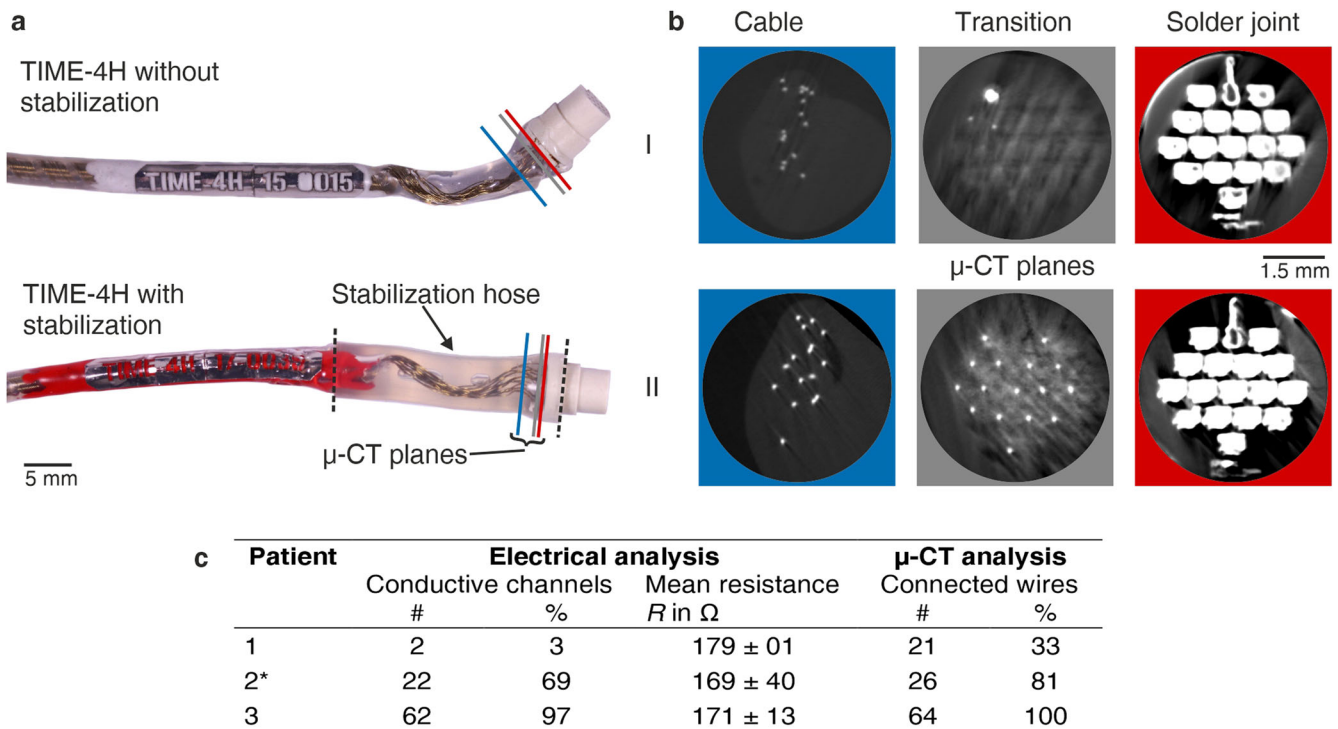
Connector analysis

After the termination of the clinical trials, the TIME implants were explanted in order to analyze the mechanical integrity of the devices. The electrical analysis of the connectors (by measuring the resistance between the connector and solder pad on the

a

b

Category	Light microscopy w. polarization filter	White light interferometry 2D h in µm 3D	Scanning electron microscopy
1			
2			
3			
4			
5			

c

Category	Mean imp. in kΩ	Standard deviation in kΩ	Median imp. in kΩ	No. of imp.	Available imp. in %	No. of not available imp.
1	76	± 35	67	26	29	6
2	58	± 18	52	8	9	4
3	79	± 47	59	40	44	7
4	46	± 38	50	7	7	1
5	68	± 44	63	10	11	2

d

VI   TIME-4H | 17-0058, RGND

interconnecting ceramic) from patient 1 revealed that only two out of 64 channels (4 implants with 14 stimulation and 2 ground channels each) were electrically conductive (with a resistance of 178 Ω and 180 Ω, respectively). All other wires were broken close to the connector. Cutting the connector and measuring between the wires and the solder pads showed that all channels except one were electrically conductive and exhibited a resistance of 175 Ω ± 10 Ω. µ-CT analysis revealed 21 connected wires to the connector.

Electrical analysis of two connectors from patient 2 revealed that 22 out of 32 channels were electrically conductive. The mean

Fig. 4 Optical thin-film analysis after explantation. a Distribution of impedances measured on the last day of use within the defined states of the metallization integrity. Box plots corresponding to the categories containing the mean (small box), median (bar) and the quartiles were generated. The numbers marked with a star represent not available impedances, n corresponds to the available impedances used for analysis. There was no statistically significant difference between the impedances of the categories at the α-level of 0.05 (Kruskal-Wallis). **b** Acquisition samples of the optical thin-film analysis, using light microscopy, white light interferometry (WLI) and scanning electron microscopy (SEM) in combination with focused ion beam (FIB). Five categories were defined for the state of metallization integrity. Category 1 represents no impact and category 5 the highest. **c** Acquired impedance data from last day of the clinical trial, referred to the categorization of the optical analysis. **d** Detailed SEM images of stimulation and ground contacts, with different failure origins like bending (dI), mechanical impact by scalpel (dII), no impact (dIII), crack formation (dIV) and crack formation from elevated in vitro stimulation with 4.5 billion pulses (dV). Overview of an explanted split ground used in patient 3 indicating crack formation with partial delamination (red stars) and only crack formation (blue triangles) (dVI). This ground contact was electrically functional after explantation.

Patient	Electrical analysis			μ-CT analysis	
	Conductive channels		Mean resistance	Connected wires	
	#	%	R in Ω	#	%
1	2	3	179 ± 01	21	33
2*	22	69	169 ± 40	26	81
3	62	97	171 ± 13	64	100

Fig. 5 Analysis and stabilization of the wire-connector transition. a The upper connector part of the TIME implant has no stabilization incorporated as used for patient 1 and 2. Below, a stabilization hose was added to the transition between wires and connector for strain relief. The μ-CT planes for integrity analysis were labeled according to the color code in (**b**). **b** μ-CT images representing a connector with ruptured wires and mechanically integer at transition. **c** Electrical and μ-CT analysis of the wire-connector transition part. The resistance was measured from the connector to the interconnecting ceramic. *Only two connectors were available for analysis after the explantation of the devices from patient 2.

resistance was at 169 Ω ± 40 Ω. Ten wires were broken. According to the μ-CT analysis, 26 wires were connected to the connector, which corresponds to 81%.

Within the retrieved implants from patient 3 with reinforced transition between wires and connector 62 out of 64 channels were still electrically conductive during electrical analysis. The channels exhibited a mean resistance of 171 Ω ± 13 Ω. μ-CT analysis revealed 64 wires were connected to the connector, which corresponds to 100%. In Fig. 5 all results of the electrical and μ-CT analysis of the connectors were summarized.

DISCUSSION

With the development of the TIME-3H using incorporated SIROF stimulation and ground contact sites, we demonstrated in a previously performed first-in-human clinical trial the feasibility of PI-based TIME implants as highly selective PNIs, capable providing for 30 days sophisticated sensory feedback to upper limb amputees[1,32]. After termination of the clinical trial and explantation of the devices, weak points were identified, solved by

introduction of adhesion promoting layers and validated in a small animal model[33]. This led to the following questions: Can neural PI-based thin-film electrodes be implanted long-term and remain mechanically intact? Will impedances be stable during a chronic implantation and will the devices elicit stable sensations? Newly developed generations of TIME implants were thoroughly analyzed after six months of human clinical trials to answer these questions and to identify issues and direct action for subsequent patients.

In order to decrease intrinsic stress in the metallization layer of the previously used rectangular large-area ground contact sites, we split it into 109 hexagonally arranged circular contact sites, which were redundantly connected between the PI layers to achieve a sufficiently large area. Simulated stress levels were comparable to calculated ones in a similar work of Ordonez[33,37]. At the revealed metallization the stress levels were increased in both types of ground contact sites as there is no upper PI layer fixing the metallization. Near the PI edges intrinsic stress was up to three times higher than in the low-stress middle of the contact sites. Particularly for the rectangular large area ground contact of the

TIME-3H this led to a continuous high stress over the whole length of the contact near the edge. This is a potential risk for delamination, which was also observed by us in an earlier study[33]. The split ground contact exhibited similar peak stress levels, but very local, which was confirmed by the integration of the intrinsic stress over the same length.

Optical analysis post explantation showed, that the state of the split ground contacts was massively improved compared to the rectangular ground contacts used sub-chronically[33]. Although some single contacts of the grounds exhibited slight crack formation and / or delamination and mechanical impact like deformation caused by surgical forceps, this had no influence on the electrochemical characteristics of the ground contact sites, as all 109 contacts were redundantly connected to each other. The split ground contact proved to be stable throughout the chronic application.

Throughout the course of the six-month clinical trial with patient 1 we observed impedances around 100 kΩ. The percentage of electrically working stimulation contacts dropped to a level of 50%. After week 22 we observed by pushing the cable of the implants towards the connector a regaining of the electrical contact, which lowered the impedance to values similar to those before week 22. Due to frequent connection and disconnection of the implants to the extracorporeal stimulator, the implants failed on the transition part between the wires of the cable and the connector. This was confirmed by the post-explantation electrical and μ-CT analysis (Fig. 5). The differences between the electrical and μ-CT analysis can be explained by limitation of the μ-CT resolution of 25 μm. Similar lead breakage failures were described by other groups[26].

The connector problem was discovered during the study with patient 2 (Fig. 5) and measures (stabilization and strain relief of the wire-connector transition) could be applied. Therefore, we observed for patient 2 a similar failure rate compared to patient 1 including high impedance slopes as well. However, the modified wire-connector transition applied for the devices in patient 3 improved the performance significantly. The mean impedance was throughout the course of the clinical trial way below 100 kΩ accompanied by a very low slope of the regression curve (Fig. 3a). The number of contacts eliciting sensation stayed very stable,

indicating that the thin-film has grown in the nerve very well, preventing displacement of the electrode[38]. The analysis of the wire-connector transition showed that 97% of the channels were electrically conductive during and after the clinical trial. We had the possibility to analyze a thin-film metallization electrically after chronic implantation post-explantation in vitro. The electrochemical characteristics remained identical to prior implantation (Fig. 3b). The shift to lower impedance could be explained by the cut cable due to safety reasons during explantation and therefore a reduction of the access resistance. After six months, no signs of corrosion were determined within the SIROF contact layer.

We classified the impedances recorded close to the explantation of the TIMEs after optical analysis postexplantation in different categories. Category 1 represented stimulation contact sites with a pristine appearance, category 5 represented the highest impact of destruction with heavy delamination of >6 μm, disintegration of the metallization layers or compression or destruction of the PI substrate. The categorized impedances displayed no statistically significant difference. The majority with 82% of the impedances were in category 1-3 with no or only low mechanical damage. Only 11% of the impedances were classified in category 5. However, externally caused mechanical damage by handling was identified in 83% of these contacts as failure cause, indicated by groove marks following bending and scratches from heavy mechanical impact like scalpels (Fig. 4d). This strengthens our presumptions made in our previous work, analyzing the implants from the first-in-human subchronical trial where more than 60% of the analyzed stimulation contacts and 100% of the ground contacts delaminated[33]. The thin-film parts of the implants were tightly encapsulated by surrounding tissue due to foreign body reaction[29] (Fig. 6a). Consequently, the thin-film experienced the highest pulling and bending forces during explantation (Fig. 6b). Neural implants either need to be removed after their end of life or are intentionally left in place if they do not harm the target tissue. Similar to some vagus nerve electrodes, TIMEs shall be left inside the nerves in future medical devices when failure occurs. The risk of nerve damage during explantation is larger than leaving the thin-film part in the nerve. The safety of the patient and the nerves must have always the highest priority, not the integrity of the TIMEs for potential ex vivo investigations. Several cuts had to be
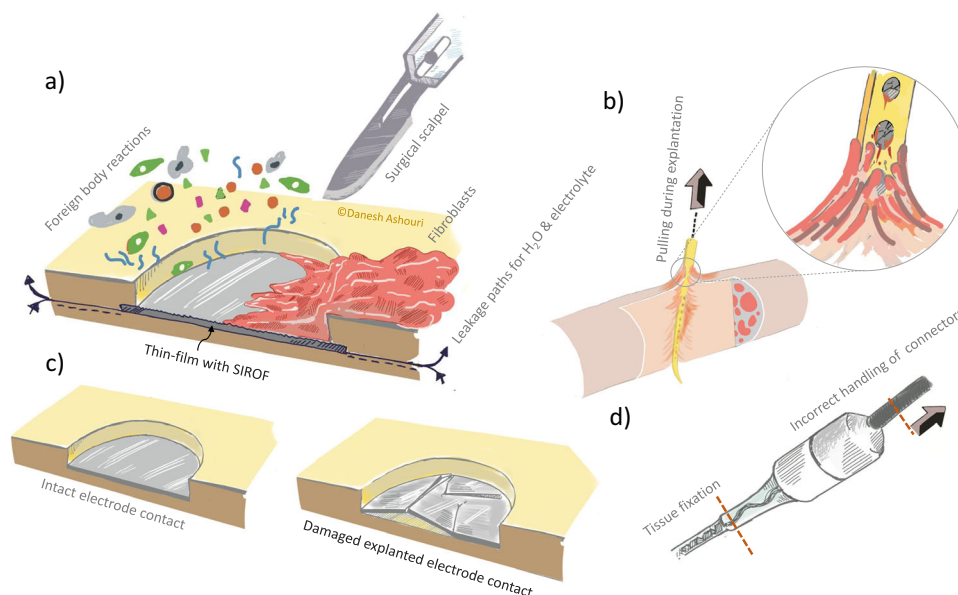
Fig. 6 Illustration of various implant situations. a The polyimide-based thin-film devices are exposed to foreign body reactions and related thereto surrounded by various cells and other tissue. **b** While pulling the thin-film out of the nerve, the thin-film experienced forces which could lead to delamination and crack formation (**c**) of the thin-film metallization. **d** Moreover, the connector parts of the devices experienced wrong handling, by pulling at the cable instead of holding the connectors themselves and pulling them apart.

made to retrieve the implants in pieces, thus the evaluation had to be performed on fragments of the devices (Fig. 1). The pulling and bending forces during explantation contributed to the observed crack formation and delamination of the metallization (Fig. 6c). We believe, that this was not induced by the electrical stimulation as we already showed in previous in vitro studies that thin-film electrodes with SIROF did not show any alteration after two billion stimulation pulses[39]. In order to confirm this, we applied 6.5 billion pulses in a further in vitro study. Here within the observed crack formation after 4.5 billion stimulation pulses, which corresponds to about 6.6 years of stimulation in chronic human application (daily use of 16 h per day with clinical relevant parameters results in $1.86 \cdot 10^6$ pulses per day), differed from the electrodes used in the human clinical trial substantially. Trident cracks of about 20 μm in length were generated within the iridium oxide film, causing a delamination of it from the underlying platinum metallization. Category 3 from the explanted electrode analysis showed cracks along the entire stimulation contact. No other morphological changes of the SIROF could be observed within all categories, indicating SIROF is an electrochemically stable material interfacing neural tissue.

METHODS

Experimental design

The objective of this study was to increase the long-term stability of thin-film-based intraneural electrodes eliciting sensation in human arm nerves and to the analyze their performance and integrity after up to six month of application.

Design considerations of the thin-film electrodes

The design of the thin-film TIME passed through various changes in its applications since the very first idea in 2008 (Fig. 7). From the early in vitro and acute in vivo experiments in rats with the TIME-1, we rapidly learned some basic pre-requisites of implantation and fixation which were implemented within the further small and large animal implants TIME-2 and TIME-3, respectively.

The implant version TIME-3H proved feasibility as an adequate peripheral nerve interface used for sensory feedback during the first sub-chronic human clinical trial[1,32]. The clinical outcome and the electrical stability of the implants were excellent. Due to explantation and subsequent handling of the thin-film electrodes, weak points were identified, especially concerning the mechanical integrity of the rectangular ground contact sites. As a first consequence, silicon carbide was introduced as an adhesion-promoting layer between the PI and platinum. This updated layer setup was tested and verified in vitro[40] and in vivo (small animal model) with regard to chronic application[33].

In order to improve the thin-film electrodes towards chronic implantation up to six months in humans, we made also some design considerations to lower intrinsic stress in the thin-film metallization, and thereby the risk of delamination, thus increasing the safety for the patient.

The TIME-3H[14,33] was consistently further developed up to the design freeze for the chronic human implantations, keeping fundamental design elements and changing details to improve the mechanical stability. The fundamental design elements were the two-dimensional U-shape for fabrication, which is transformed into a L-shape after folding during assembly. Details are described elsewhere[14,33]. Further fundamental design elements were realized with the thin-film sectioning. It consisted of three parts: the electrode, ribbon and transition part (Fig. 8a). The electrode part contained the active strip with 14 stimulation sites incorporated (seven per side) and after folding a loop with an integrated surgical needle and thread. Positioning, pitch and size of the stimulation contact sites were depending on the thin-film version. The sti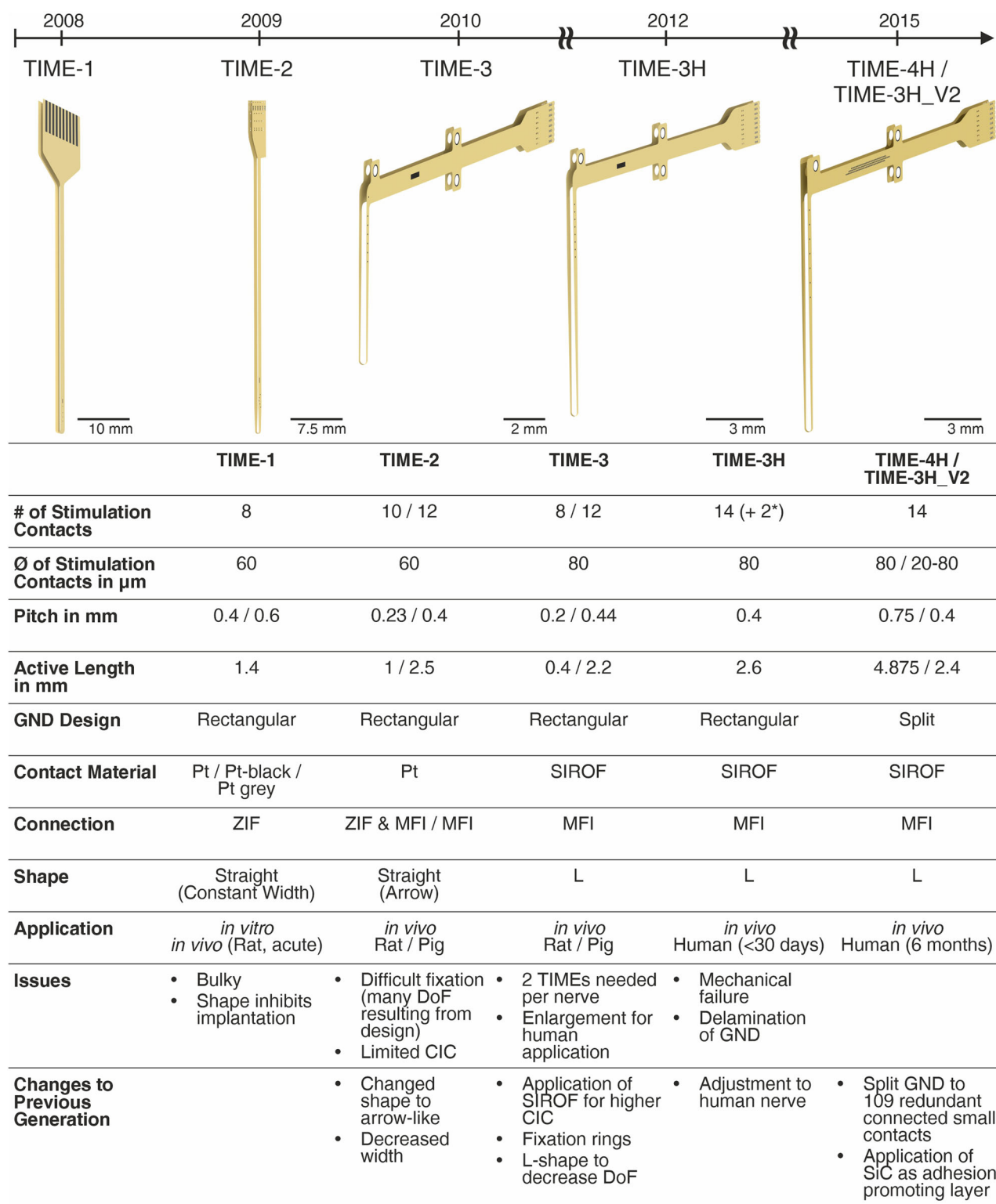mulation contact sites were labeled from the ribbon part towards the middle line L1 to L7 and R1 to R7 (Fig. 8a). The ribbon part contained all tracks, which led from the transition part to the stimulation contact sites and the large area ground sites, named L GND and R GND. The transition part had incorporated a structure to interconnect the thin-film electrode with a subsequent helically wound cable. The Microflex interconnection technique (MFI)[41] was used as a robust and reliable technique to assemble a thin-film ribbon with a long helically wound cable (Fig. 8a). The focus of the current designs was placed on the large electrode area of the ground contact sites (see simulation sections). The ground contact sites are of fundamental importance, as a failure would lead to a total malfunction of the implant. The aim of the redesign was to prevent stress due to the large continuous area and rectangular edges, but to keep an area as large as possible to ensure an electrical closed-loop for stimulation. To preserve these boundary conditions, the rectangular ground site was split to 109 interconnected circular contacts with an exposed diameter of $d = 80$ μm (Fig. 8a, red box) (diameter under polyimide $d = 100$ μm) of a single site. The contacts were arranged in a hexagonal assembly with a pitch of 125 μm in three rows. Eliminating large continuous areas and replacing highly stressed rectangular edges by round shapes should decrease the intrinsic stress of the thin-film metallization and thus decreasing the risk of delamination. A further advantage of the design, in case of partial damage, was the structural resilience of the design. The remaining ground contact sites would be still functional as every contact of the ground is electrically connected among each other. Concerning the active strip, two designs were developed, resulting in the TIME-3H_V2 and the TIME-4H. Both were manufactured with the split ground contact sites.

The TIME-3H_V2 was conceptualized in a way, that the left side of the electrode had integrated seven standard active sites with a diameter of 80 μm. However, the right side exhibited from the ribbon part downwards on the active strip decreasing the diameters of the active sites. The diameter started at 60 μm and decreased with 20 μm steps down to a diameter of 20 μm and starting again at 60 μm. In the folded state, the active sites were directly opposite to the left side. The active strip had a length of 2.4 mm, resulting in a contact site pitch of 0.4 mm.

The design of the active strip within the TIME-4H was developed in way to cope a larger area / diameter of the targeted nerve with a single electrode, as for this type of implant the surgical protocol was slightly different[42]. Considering that using directly opposite stimulation sites would mean one fascicle is addressed by two active sites, a shift of half the pitch (in this case 0.75 mm) of left and right side of the electrode was included to potentially address more fascicles with the same number of active sites. Otherwise the standard size for the active sites of 80 μm in diameter was used.

In both versions, platinum tracks and pads were sandwiched between polyimide as substrate and insulation layer (Fig. 8b). Silicon carbide (SiC) was used as an adhesion promoter between platinum and the PI substrate. Platinum tracks were completely surrounded by the SiC and polyimide (details below). At the active sites and ground contacts, the platinum layer was coated by iridium, subsequently covered by a sputtered iridium oxide film (SIROF) and opened via reactive ion etching (RIE). The MFI structure exhibited SiC only between platinum and the lower PI layer, in order to have bare platinum on the MFI ring after RIE opening for mechanical adhesion within the assembly procedure.

The detailed implantation procedure is described elsewhere[1,14]. In general, the front part of the TIME design (active part) is pulled with the incorporated needle and suture during the implantation through the nerve. The active sites for stimulation have to lay inside the nerve. The fixation flaps and the loop are sutured to the surrounding tissue, for the purpose of avoiding movements of the electrode during daily life.

	TIME-1	TIME-2	TIME-3	TIME-3H	TIME-4H / TIME-3H_V2
# of Stimulation Contacts	8	10 / 12	8 / 12	14 (+ 2*)	14
Ø of Stimulation Contacts in µm	60	60	80	80	80 / 20-80
Pitch in mm	0.4 / 0.6	0.23 / 0.4	0.2 / 0.44	0.4	0.75 / 0.4
Active Length in mm	1.4	1 / 2.5	0.4 / 2.2	2.6	4.875 / 2.4
GND Design	Rectangular	Rectangular	Rectangular	Rectangular	Split
Contact Material	Pt / Pt-black / Pt grey	Pt	SIROF	SIROF	SIROF
Connection	ZIF	ZIF & MFI / MFI	MFI	MFI	MFI
Shape	Straight (Constant Width)	Straight (Arrow)	L	L	L
Application	*in vitro* *in vivo* (Rat, acute)	*in vivo* Rat / Pig	*in vivo* Rat / Pig	*in vivo* Human (<30 days)	*in vivo* Human (6 months)
Issues	• Bulky • Shape inhibits implantation	• Difficult fixation (many DoF resulting from design) • Limited CIC	• 2 TIMEs needed per nerve • Enlargement for human application	• Mechanical failure • Delamination of GND	
Changes to Previous Generation		• Changed shape to arrow-like • Decreased width	• Application of SIROF for higher CIC • Fixation rings • L-shape to decrease DoF	• Adjustment to human nerve	• Split GND to 109 redundant connected small contacts • Application of SiC as adhesion promoting layer

* Two not electrically connected
GND = Ground; MFI = Microflex Interconnection; Pt = Platinum; TIME = Transverse Intrafascicular Multichannel Electrode;
SIROF = Sputtered Iridium Oxide Film; ZIF = Zero Insertion Force

Fig. 7 Design history of the TIME implants. TIME-2 was mostly used in small animal experiments, proving biocompatibility of the used materials[29] and showing advantages in the stimulation selectivity[19]. TIME-3 implants were used mainly in large nerves of pigs[30,31]. SIROF was applied as contact material to increase the charge injection capacity and thus increase the stimulation safety limits[14,45]. In a first-in-human study the TIME-3H showed excellent clinical outcomes[1,32], but as well weak points concerning the mechanical integrity, especially of the ground contact sites[33]. SiC was introduced as adhesion promoting layer and the large area ground contact site was split into 109 redundant connected small contact sites.
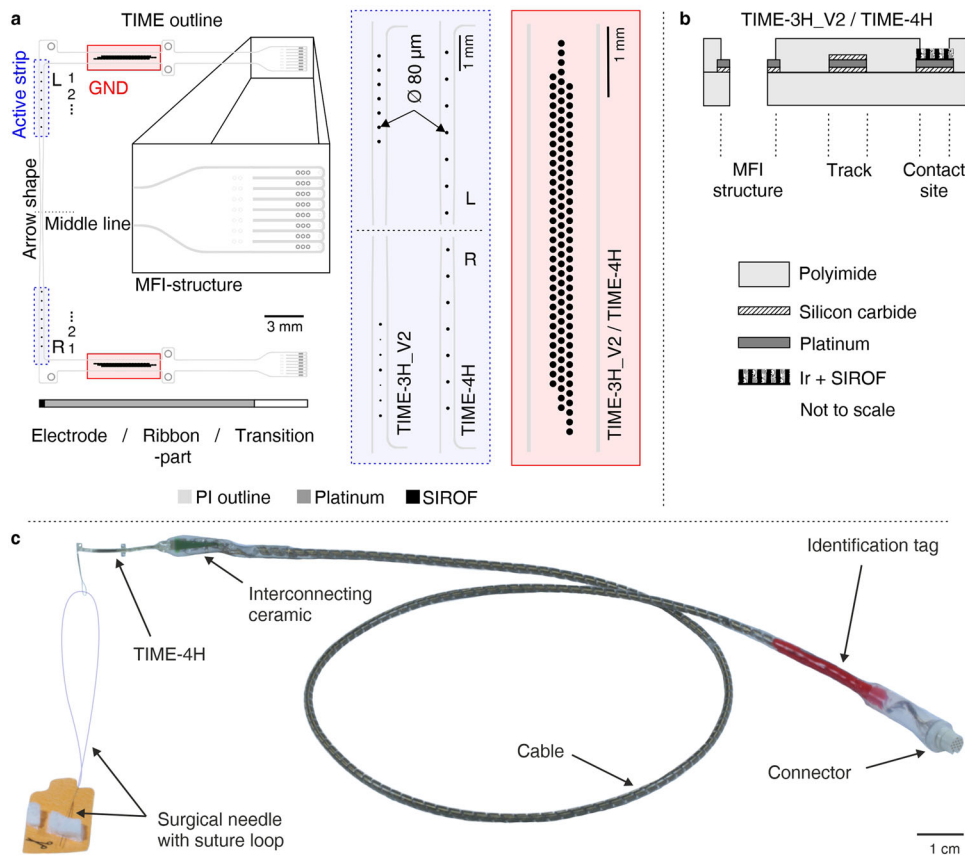
Fig. 8 Overview of the different TIME designs. a Two different designs for the active strips were realized (blue box). The ground contact site was split to 109 circular redundant connected contacts with a single diameter of 80 μm (red box). **b** The layer setup of both designs was chosen identical. **c** In the assembled TIME implant a surgical needle with a suture was incorporated within the thin-film loop (TIME-4H). The polyimide-based thin-film electrode was attached via the MFI technique to an interconnecting by use of screen-printing structured ceramic. To this in turn 16 helically wound MP35N- wires covered by a medical-grade silicone rubber hose were soldered and terminated on the opposite side in a commercial connector. Colored silicone rubber and an identification tag made of laser-structured platinum were used for distinct identification.

Simulation of intrinsic mechanical stress

Thermo-mechanical intrinsic stress was simulated using COMSOL Multiphysics® (version 5.3, COMSOL Inc., Burlington, MA, USA). If not otherwise stated, standard parameters given by the software were applied.

Two concepts of the large area ground contacts were designed. First, a rectangular design used for the TIME-3H[14,33], i. e. with an exposed metallization area of 1 mm × 0.25 mm ($A = 0.25$ mm²) and second, a split ground with 109 circular exposed metallization contacts with a diameter of $d = 0.08$ mm ($A = 0.55$ mm²). For simplification, a polyimide-platinum sandwich was simulated without adhesion layers and without SIROF. Platinum is the main conductive material, representing the tracks, MFI structures and the base of the stimulation and contact sites. If failure occurs within the platinum structure, the whole device is prone to failure.

Minimizing the intrinsic stress in the platinum layer is of the highest relevance. SIROF however serves only as enhancement of the charge transfer to the tissue.

The geometries were designed in SolidWorks (Version 2014, Dassault Systemes Deutschland GmbH, Stuttgart, Germany) and imported in COMSOL Multiphysics®. Parameters of both materials, polyimide and platinum were acquired via the internal "MEMS" materials library (changed parameters are listed in Fig. 2c). Several boundaries from the "Solid Mechanics" and "Heat Transfer in Solids" from the internal definitions were applied. An external temperature of 394.15 K as heat flux boundary was chosen according to the sterilization process performed after assembly

(not 723.15 K imidizing temperature, since the metallization is homogeneously sandwiched between closed PI layers within this process step). A free tetrahedral mesh was used with custom-changed mesh sizes.

Cleanroom fabrication of thin-film electrodes

The microfabrication of the TIME thin-film electrodes was conducted in a cleanroom environment using standard photo-lithographic and MEMS processes (Supplementary Fig. 1). Details are described in the supplementary material and elsewhere[14,33]. All thin-film electrode designs described above feature polyimide (PI; type: biphenyldianhydride / 1,4-phenylenediamine BPDA-PPD) as substrate and insulation material. MEMS processes utilized were plasma-enhanced chemical vapor deposition of SiC (PECVD, PC310 reactor by SPS Process Technology Systems Inc, San Jose, CA, USA), evaporation of Pt (Leybold Univex 500, Leybold Vacuum GmbH, Cologne, Germany) and sputter deposition of Ir and IrO$_x$ (Leybold Univex 500, Leybold Vacuum GmbH, Cologne, Germany). After the last fabrication step, the thin-film electrodes were pulled off the silicon wafer with a pair of forceps (Supplementary Fig. 1g) for assembly of the implants.

Chronic human implant

The TIME-3H_V2 and TIME-4H implants (called TIME implants if specification not relevant) were assembled out of four sub-modules (Fig. 8c; for details see[14]). First, the thin-film part

containing the contact sites for stimulation and the ground contacts to close the electrical circuit. Second, a screen-printed interconnecting ceramic to mechanically and electrically connect the thin-film electrode to the third part, a 40 cm long cable. The fourth module was a commercially available connector (NCP-16-DD, Omnetics Connector Corporation, Minneapolis, USA).

The fabrication procedure was similar to the fabrication procedure of the TIME-3H (details in[14,33]) with little adjustments due to chronic application in human (details in supplementary materials).

After some connector issues, with regard to strain relief during daily handling, loosing channels within the first two patients[7] the connector assembly was strengthened using a protective rubber hose (NuSil MED-4750, Freudenberg Medical Europe GmbH, Kaiserslautern, Germany) at the wire-connector transition (Fig. 8c) for patient 3.

The TIME implants were fabricated within the fully ISO 13485-certified Laboratory for Biomedical Microtechnology of the Albert-Ludwig-University of Freiburg, Freiburg, Germany. Before implantation, each TIME was hydrated in order to increase the charge injection capacity[43], characterized and tested on functionality. Afterwards, it was washed, wrapped in sterile bags, labelled and steam-sterilized at 121 °C and 2 bars for 21 minutes. The stimulation and ground contact sites of all delivered implants were fully functional.

Within clinical trials, MRI investigations are of interest and therefore the state of MRI compatibility of implants is relevant[44]. Medical devices can be declared according to the ASTM standard F2503 MR safe, MR conditional and MR unsafe. We have used the F2503-08 version while the F2503-13 was released after our examinations had been finished. Investigation according to the relevant standards (ASTM F2052-14, F2213-06 & F2182-11a) have demonstrated that the TIME-4H implants (in clinically relevant position and orientation according to manufacturer specification) can be considered "MR conditional". Meaning, a patient with these devices can be safely scanned in a MR system meeting the following conditions; 1) static magnetic field of 3 T, with 2) maximum spatial field gradient of 25700 Gcm^{-1} (257 Tm^{-1}) and 3) maximum force product of 441 T^{2}m^{-1}.

Under the scan conditions defined above, the TIME-4H electrode is expected to produce a maximum temperature rise of <0.5 °C (2.3 Wkg^{-1}, 3 T) RF-related (switched gradient during imaging) temperature increase with a background temperature increase of <0.1 °C (2.3 Wkg^{-1}, 3 T).

Human clinical trials
Human clinical trials were performed in three patients according to European Law between 2015 and 2017. This study was conducted as part of the clinical trial NCT02848846 (https://clinicaltrials.gov/). Electrodes were explanted at the end of the trial periods. Details are described in the supplementary material.

Electrochemical electrode characterization
In order to compare the electrochemical properties of the TIMEs before implantation and after explantation the devices underwent a characterization with electrochemical impedance spectroscopy (EIS) in vitro. The characterization was carried out with a frequency analyzer and a potentiostat (SI 1260 & SI 1287, Solartron Analytical, Farnborough, UK) in phosphate-buffered saline (PBS) solution with a voltage amplitude of 10 mV and a frequency range of 100 kHz to 1 Hz. The three-electrode setup consisted of an Ag/AgCl reference, a large area platinum counter and the respective stimulation or ground contact sites of the TIME implant as working electrode. Beforehand, the SIROF was hydrated via cyclic voltammetry[43], using the identical setup as used within EIS. The voltage sweep was performed between −0.6 V and 0.8 V, with 200 mV steps for 250 cycles.

Three neural stimulators: STIMEP (INRIA, Montpellier, France & Axonic, Vallauris, France), EARNEST (University of Cagliari, Italy) and the Grapevine Neural Interface System (Neural Interface Processor, 512 Channels of Potential, Ripple LLC, Salt Lake City, UT, USA) were used to inject current into the nerves of the subjects by means of TIME implants (details are provided in the supplementary materials). For the characterization of the electrode-nerve impedance in vivo and the subjects' response to intraneural stimulation, we delivered trains of cathodic-first, biphasic and symmetric square-shaped, current-controlled stimulation pulses of variable intensity, duration, and frequency, through a dedicated software controlling one of the before mentioned, external, electrical neural stimulators. The impedance in vivo was estimated as the ratio between the potential difference between the selected stimulation contact site and the ground contact sites (both, left and right one of the electrode) at the end of the cathodic pulse phase divided by the current pulse magnitude. The potential resulted from the average of four pulses (the first one of a five-pulse train was removed) with a current amplitude of 20 µA and a pulse width of 300 µs, repeated at a frequency of 1 Hz. While a safety margin has been applied in functional assessment in the patients[7], this paper uses 150kΩ as maximum impedance for the definition of electrically functional stimulation contact sites which corresponds to the maximum output swing of the stimulators.

Optical analysis of explanted thin-film electrodes
The optical analysis of the stimulation and ground contact sites were done using light microscopy with polarization filters (Leica DM400M, Leica Microsystems GmbH, Wetzlar, Germany) to enhance visualization of surface irregularities and changes in adhesion (Fig. 4b, left column).

White light interferometry (WLI; Wyko NT9100, Veeco Instruments Inc., Plainview, NY, USA) was used to quantitatively investigate the topography in three dimensions (Fig. 4b, middle columns).

In accordance to analyze the properties of the layer setup, scanning electron microscopy (SEM) in combination with focused ion beam (FIB; Zeiss Auriga 60, Carl Zeiss AG, Oberkochen, Germany) was utilized to gather high-resolution overviews of the contact sites and to cut cross-sections into the thin-film metallization.

Five categories of stimulation contact site status were defined in order to obtain an objective classification (Fig. 4b). Category 1 represents a contact which can be compared to a pristine one, meaning from a material (not electrical) point of view, fully functional, with perfect adhesion and perfect surface integrity. Category 2 exhibits signs of delamination of ≤1 µm (distance between metal and underlying polyimide substrate) and / or (possible) light crack formation in the contact site coating. Delamination between 1 µm and 6 µm and crack formation occurs in category 3. Partial delamination of a metallization layer is categorized as cat. 4. The highest impact of destruction occurs in category 5 with heavy delamination of >6 µm, disintegration of the metallization layers or compression or destruction of the PI substrate.

For comparison reasons, 15 stimulation contact sites identical to TIME stimulation contacts were stimulated using a pulse generator up to 6.5 billion times. The test was performed using a two-electrode setup. A large area platinum counter electrode and the TIME-like stimulation contacts were used as working electrodes in PBS solution, as well as a stimulator (PlexStim Electrical Stimulator, Plexon Inc. Dallas, TX, USA) and a pH-meter (pH-Meter, Qph70, VWR International GmbH, Darmstadt, Germany) to monitor the pH-value during the stimulations. A rectangular charge-balanced pulse form was applied, cathodic first with a pulse width of 200 µs, 10 µs pulse delay and a repetition frequency of 500 Hz. The amplitude was set to 578 µA which was calculated based on the

safe charge injection limit of SIROF (2.3 mCcm^{-2}) to avoid overstimulation[14]. Gathering the voltage response using a picoscope (PicoScope 2000 Series, Pico Technology, St. Neots, UK) and evaluation of its data using MATLAB (MATLAB, The MathWorks, Inc., Natick, US).

To gather compound overviews of the ground contact sites with a high degree of details, images with a tabletop SEM (Phenom Pro Desktop SEM, Thermo Fisher Scientific Phenom-World B.V., Eindhoven, Netherland) were acquired and highlighted with CorelDRAW X7 (Corel Graphics Suite X7, Corel GmbH, München, Germany).

Connector analysis
Issues with the connector assembly occurred as already mentioned above. During daily handling (connection and disconnection of the extracorporeal stimulator) many channels were lost. After scheduled termination of the clinical trial, the implants were retrieved. The connectors were analyzed with regard to the electrical state and the mechanical integrity. The electrical state was tested with a resistance meter (34401 A 6 ½ Digit Multimeter, Agilent, Santa Clara, CA, USA) between different tapping points (connector – solder pads on inter-connecting ceramic – wires anterior to interconnecting ceramic). Mechanical integrity at the wire-connector transition was investigated using μ-computer tomography (μ-CT; Nano-tom m, GE Sensing & Inspection Technologies, Wunstorf, Deutschland) (Fig. 5). Using this technique, x-ray images were acquired in all three dimensions throughout the wire-connector transition (Fig. 5b). In case of a ruptured wire from the connector there is no white dot representing the cross-section of a wire visible at the transition position (Fig. 5b, upper grey image). In the lower transition image in Fig. 5b all 16 wires a visible.

Statistical analysis
Statistical methods were applied for data analysis of the electrochemical experiments. The data acquired in vivo was longitudinal and unbalanced for each time point (weeks). Moreover, the data was not normal distributed and the variance was not homogeneous as well. Therefore, we applied a linear mixed effect model using the software R (version 3.5.2, The R Foundation for Statistical Computing, Vienna, Austria) and RStudio (Version 1.1.463, RStudio Inc., Boston, MA, USA), which is robust to non-normality and unbalanced data sets. Further detailed statistical analysis of the impedance data was performed elsewhere[7].

A non-parametric Kruskal-Wallis method was applied, to assess differences between the impedances classification, comparing optical and electrochemical data.

DATA AVAILABILITY
All data needed to evaluate the conclusions in the article are available in the main text or the supplementary materials. Additional data related to this paper may be requested from authors.

REFERENCES
1. Raspopovic, S. et al. Restoring natural sensory feedback in real-time bidirectional hand prostheses. *Sci. Transl. Med* **6**, 222 (2014).
2. Schiefer, M. A., Tan, D. W., Sidek, S. M. & Tyler, D. J. Sensory feedback by peripheral nerve stimulation improves task performance in individuals with upper limb loss using a myoelectric prosthesis. *J. Neural Eng.* **13**, 016001 (2016).
3. Pasluosta, C., Kiele, P. & Stieglitz, T. Paradigms for restoration of somatosensory feedback via stimulation of the peripheral nervous system. *Clin. Neurophysiol.* **129**, 851–862 (2018).
4. Horch, K., Meek, S., Taylor, T. G. & Hutchinson, D. T. Object discrimination with an artificial hand using electrical stimulation of peripheral tactile and proprioceptive pathways with intrafascicular electrodes. *IEEE Trans. Neural Syst. Rehabil. Eng.* **19**, 483–489 (2011).
5. Biddiss, E. A. & Chau, T. T. Upper limb prosthesis use and abandonment: a survey of the last 25 years. *Prosthet. Orthot. Int.* **31**, 236–257 (2007).
6. Biddiss, E., Beaton, D. & Chau, T. Consumer design priorities for upper limb prosthetics. *Disabil. Rehabil. Assist Technol.* **2**, 346–357 (2009).
7. Petrini, F. M. et al. Six-months assessment of a hand prosthesis with intraneural tactile feedback. *Ann. Neurol.* **85**, 137–154 (2019).
8. Valle, G. et al. Biomimetic intraneural sensory feedback enhances sensation naturalness, tactile sensitivity, and manual dexterity in a bidirectional Prosthesis. *Neuron* **100**, 37–45 (2018).
9. Clemente, F. et al. Intraneural sensory feedback restores grip force control and motor coordination while using a prosthetic hand. *J. Neural Eng.* **16**, 026034 (2019).
10. Dietrich, C. et al. Sensory feedback prosthesis reduces phantom limb pain: proof of a principle. *Neurosci. Lett.* **507**, 97–100 (2012).
11. Schiefer, M. A., Graczyk, E. L., Sidik, S. M., Tan, D. W. & Tyler, D. J. Artificial tactile and proprioceptive feedback improves performance and confidence on object identification tasks. *PLoS One* **13**, e0207659 (2018).
12. Murray, C. D. An interpretative phenomenological analysis of the embodiment of artificial limbs. *Disabil. Rehabil.* **26**, 963–973 (2004).
13. Rognini, G. et al. Multisensory bionic limb to achieve prosthesis embodiment and reduce distorted phantom limb perceptions. *J. Neurol. Neurosurg. Psychiatry* **90**, 833–836 (2019).
14. Boretius, T. et al. A transverse intrafascicular multichannel electrode (TIME) to treat phantom limb pain — Towards human clinical trials. In *Proceedings of the IEEE International Conference on Biomedical Robotics and Biomechatronics (BioRob)*, 282–287 (2012).
15. Tyler, D. J. Neural interfaces for somatosensory feedback. *Curr. Opin. Neurol.* **28**, 574–581 (2015).
16. Ortiz-Catalan, M., Håkansson, B. & Brånemark, R. An osseointegrated human-machine gateway for long-term sensory feedback and motor control of artificial limbs. *Sci. Transl. Med* **6**, 257 (2014).
17. Dhillon, G. S., Krueger, T. B., Sandhu, J. S. & Horch, K. W. Effects of short-term training on sensory and motor function in severed nerves of long-term human amputees. *J. Neurophysiol.* **93**, 2625–2633 (2005).
18. Rossini, P. M. et al. Double nerve intraneural interface implant on a human amputee for robotic hand control. *Clin. Neurophysiol.* **121**, 777–783 (2010).
19. Badia, J. et al. Comparative analysis of transverse intrafascicular multichannel, longitudinal intrafascicular and multipolar cuff electrodes for the selective stimulation of nerve fascicles. *J. Neural Eng.* **8**, 036023 (2011).
20. Tyler, D. J. & Durand, D. M. Functionally selective peripheral nerve stimulation with a flat interface nerve electrode. *IEEE Trans. Neural Syst. Rehabil. Eng.* **10**, 294–303 (2002).
21. Tyler, D. J. & Durand, D. M. Chronic response of the rat sciatic nerve to the flat interface nerve electrode. *Ann. Biomed. Eng.* **31**, 633–642 (2003).
22. Tan, D. W. et al. A neural interface provides long-term stable natural touch perception. *Sci. Transl. Med* **6**, 257 (2014).
23. Campbell, P. K., Jones, K. E., Huber, R. J., Horch, K. W. & Normann, R. A. A silicon-based, three-dimensional neural interface. Manufacturing processes for an intracortical electrode array. *IEEE Trans. Biomed. Eng.* **38**, 758–768 (1991).
24. Wise, K. D., Angell, J. B. & Starr, A. An integrated-circuit approach to extracellular microelectrodes. *IEEE Trans. Biomed. Eng.* **17**, 238–247 (1970).
25. Davis, T. S. et al. Restoring motor control and sensory feedback in people with upper extremity amputations using arrays of 96 microelectrodes implanted in the median and ulnar nerves. *J. Neural Eng.* **13**, 036001 (2016).
26. Barrese, J. C. et al. Failure mode analysis of silicon-based intracortical microelectrode arrays in non-human primates. *J. Neural Eng.* **10**, 066014 (2013).
27. Barrese, J. C., Aceros, J. & Donoghue, J. P. Scanning electron microscopy of chronically implanted intracortical microelectrode arrays in non-human primates. *J. Neural Eng.* **13**, 026003 (2016).
28. Boretius, T. et al. A transverse intrafascicular multichannel electrode (TIME) to interface with the peripheral nerve. *Biosens. Bioelectron.* **26**, 62–69 (2010).
29. Badia, J. et al. Biocompatibility of chronically implanted transverse intrafascicular multichannel electrode (TIME) in the rat sciatic nerve. *IEEE Trans. Biomed. Eng.* **58**, 2324–2332 (2011).
30. Harreby, K. R. et al. Subchronic stimulation performance of transverse intra-fascicular multichannel electrodes in the median nerve of the Göttingen minipig. *Artif. Organs* **39**, E36–E48 (2015).

31. Kundu, A. et al. Stimulation selectivity of the "thin-film longitudinal intrafascicular electrode" (tfLIFE) and the "transverse intrafascicular multi-channel electrode" (TIME) in the large nerve animal model. *IEEE Trans. Neural Syst. Rehabil. Eng.* **22**, 400–410 (2014).

32. Oddo, C. M. et al. Intraneural stimulation elicits discrimination of textural features by artificial fingertip in intact and amputee humans. *Elife* **5**, e09148 (2016).

33. Čvančara, P. et al. Stability of flexible thin-film metallization stimulation electrodes: analysis of explants after first-in-human study and improvement of in vivo performance. *J. Neural Eng.* **17**, 046006 (2020).

34. Granata, G. et al. Phantom somatosensory evoked potentials following selective intraneural electrical stimulation in two amputees. *Clin. Neurophysiol.* **129**, 1117–1120 (2018).

35. Valle, G. et al. Comparison of linear frequency and amplitude modulation for intraneural sensory feedback in bidirectional hand prostheses. *Sci. Rep.* **8**, 16666 (2018).

36. D'Anna, E. et al. A closed-loop hand prosthesis with simultaneous intraneural tactile and position feedback. *Sci. Robot* **4**, eaau8892 (2019).

37. Ordonez, J. S. Miniaturization of neuroprosthetic devices and the fabrication of a 232-channel vision prosthesis with a hermetic package. *Der Andere Verlag*, Uelvesbüll; (2013).

38. Wurth, S. et al. Long-term usability and bio-integration of polyimide-based intraneural stimulating electrodes. *Biomaterials* **122**, 114–129 (2017).

39. Boretius, T. TIME. A transverse intrafascicular multichannel electrode. *Der Andere Verlag*, Uelvesbüll; (2013).

40. Ordonez, J. S., Schuettler, M., Boehler, C., Boretius, T. & Stieglitz, T. Thin films and microelectrode arrays for neuroprosthetics. *MRS Bull.* **37**, 590–598 (2012).

41. Stieglitz, T., Beutel, H. & Meyer, J.-U. "Microflex"—A new assembling technique for interconnects. *J. Intell. Mater. Syst. Struct.* **11**, 417–425 (2000).

42. Krähenbühl, S. M. et al. Return of the cadaver. Key role of anatomic dissection for plastic surgery resident training. *Medicine (Baltimore)* **96**, 29 (2017).

43. Boretius, T. & Stieglitz, T. The influence of hot-steam sterilization on hydrated sputtered iridium oxide films. In *2013 6th International IEEE/EMBS Conference on Neural Engineering (NER)*, 279–282 (2013).

44. Erhardt, J. B. et al. Should patients with brain implants undergo MRI? *J. Neural Eng.* **15**, 041002 (2018).

45. Cogan, S. F. Neural stimulation and recording electrodes. *Annu Rev. Biomed. Eng.* **10**, 275–309 (2008).

AUTHOR CONTRIBUTIONS

P.Č. designed and fabricated the TIME-4H and performed the electrical analysis of the in vivo and in vitro measurements and the optical analysis of the implants. He transferred the outcome into the manuscript and was writing the manuscript. T.S. was the co-designer of TIME-4H and TIME-3H_V2 and supervisor of this study, acted as scientific advisor and edited the manuscript. G.V., F.P., S.R., I.S., G.G., E.F., P.M.R. and S. M. performed the human clinical trial and edited the manuscript. G.V. and F.P. acquired and preprocessed impedance data. M.M. designed and fabricated the TIME-3H_V2 and edited the manuscript. I.B. performed in vitro testing. T.G., A.H., J.-L.D. and D.G. designed and manufactured the software and hardware of the stimulator STIMEP and edited the manuscript. T.G., A.H. and D.G. acquired and preprocessed impedance data. M.B. designed and manufactured the software and hardware of the stimulator EARNEST and edited the manuscript. K.Y. gave scientific advice in the clinical study and contributed in manuscript proof-reading. W.J. gave scientific advice in the clinical study and contributed in manuscript proof-reading and editing.

COMPETING INTERESTS

S.R., F.P. and S.M. hold shares and P.Č. was in an advisory position of "Sensars Neuroprosthetics", a start-up company dealing with potential commercialization of neuro-controlled artificial limbs. All other authors declare they have no competing interests.

ADDITIONAL INFORMATION

Supplementary information The online version contains supplementary material available at https://doi.org/10.1038/s41528-023-00284-x.

Correspondence and requests for materials should be addressed to Paul. Čvančara.

Reprints and permission information is available at http://www.nature.com/reprints

Publisher's note Springer Nature remains neutral with regard to jurisdictional claims in published maps and institutional affiliations.